14th International Beam Instrumentation Conference, Liverpool, UK JACoW Publishing
ISBN: 978-3-95450-262-2 ISSN: 2673-5350 doi: 10.18429/JACoW-IBIC2025-WEPCO05

DESIGN OF SPECTROMETER ENERGY MEASUREMENT SETUPS FOR THE FUTURE EUPRAXIA@SPARC_LAB AND SSRIP LINACS

D. Quartullo*, D. Alesini, F. Demurtas, L. Faillace, G. Franzini, A. Ghigo, A. Giribono, R. Pompili, L. Sabbatini, A. Stella, C. Vaccarezza, A. Vannozzi, L. Verra, INFN-LNF, Frascati, Italy
A. Cianchi, Università Tor Vergata, Rome, Italy

Abstract

EuPRAXIA@SPARC_LAB is a FEL user-facility currently under construction at INFN-LNF in the framework of the EuPRAXIA collaboration. The electron beam will be accelerated to 1 GeV by an X-band RF linac followed by a plasma wakefield acceleration stage. This high-brightness linac requires diagnostic tools able to measure the beam parameters with high accuracy and resolution. To monitor the beam energy and its spread, magnetic dipoles and quadrupoles will be installed along the linac, together with viewing screens and CCD cameras. Macroparticle beam dynamics simulations were performed to determine the optimal energy measurement setup in terms of accuracy and resolution. Similar diagnostics evaluations were carried out for the spectrometer installed at the 100 MeV RF linac of the beam facility SSRIP (IFIN-HH, Romania), whose commissioning planned for 2026 will be performed by INFN-LNF in collaboration with IFIN-HH. Optics measurements were performed to characterize the resolution and magnification of the optical system foreseen to be used at EuPRAXIA@SPARC_LAB and SSRIP for beam energy monitoring.

INTRODUCTION

EuPRAXIA@SPARC_LAB is a multi-disciplinary user-facility under construction at INFN-LNF [1, 2]. It is composed of an X-band photoinjector and linac, a discharge plasma capillary and a FEL undulator. The high-brightness linac requires diagnostics tools able to measure with high accuracy and resolution the electron beam parameters along the machine. The beam energy monitoring is important for instance at the exit of the plasma module to quantify the energy jitter, which is the dominant source of the FEL performance instability. Beam energy measurements will be also needed at the beam facility SSRIP (IFIN-HH), based on an RF linac accelerating electron bunches to 100 MeV.

Spectrometers are commonly used in linacs to measure the beam energy and its rms [3–8]. Each spectrometer is a dipole magnet which disperses the beam by energy in the horizontal plane. Quadrupole magnets installed before the dipole focus the beam onto a viewing screen placed after the dipole. From the beam spot at the screen, the energy profile is estimated. The magnets and the screen should be designed to have the desired energy resolution and accuracy. Macroparticle simulations can help significantly for this task.

In this paper, the energy-measurement design is presented for EuPRAXIA@SPARC_LAB and SSRIP. The last section describes the characterization of the optics system which will be used at these accelerators to acquire the beam spots.

* danilo.quartullo@lnf.infn.it

DESIGN OF ENERGY MEASUREMENTS FOR EUPRAXIA@SPARC_LAB

Three spectrometers will be installed along the beamline (Fig. 1, top): downstream of the photoinjector and before the first linac (120 MeV), after the bunch compressor and before the second linac (400 MeV), after the plasma module and before the undulator (1 GeV). For each spectrometer,

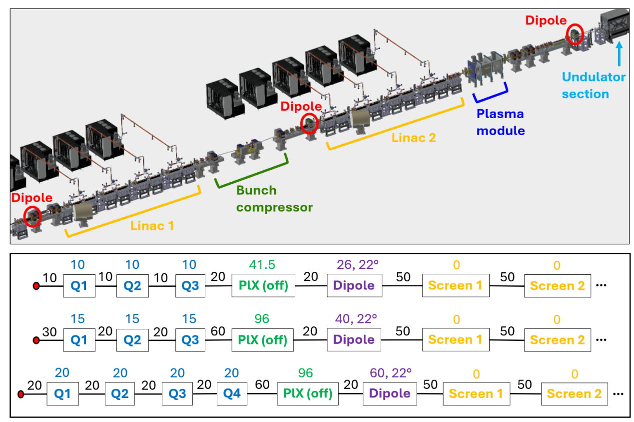

Figure 1: Top: part of the CAD layout of the accelerator EuPRAXIA@SPARC_LAB. The first spectrometer is rectangular (first magnet of the laser-heater chicane), the other two are sector dipoles. Bottom: lattice schemes assumed in the simulations, at 120 MeV (top), 400 MeV (middle) and 1 GeV (bottom). The numbers are lengths in centimeters. The red dots indicate where simulations start. The quadrupoles are in blue. The PolariX RF structures (green) are switched off during the energy measurements. Dipole arc length and bending angle are in purple. After each dipole, the beam spot is analyzed at six evenly-spaced positions ('screens').

macroparticle simulations were performed with the Elegant code [9] to determine where to position the screen (Fig. 1, bottom). The initial beam distributions were obtained from separate macroparticle simulations [2]. The quadrupole strengths found with the MAD-X code [10] minimized the beta function β_x at the screen. The quadrupole strengths were below the limits set by the maximum quadrupole gradients. The macroparticle transverse displacements up to the dipole were lower than the smallest half aperture of the lattice. The magnification was chosen as low as possible to maximize the energy resolution at the screen, while avoiding

ISBN: 978-3-95450-262-2 ISSN: 2673-5350 doi: 10.18429/JACoW-IBIC2025-WEPCO05

that more than 0.02 % of the macroparticles was out of the field of view (FOV). A camera sensor with 1920 × 1200 pixels, and pixel side of 3.45 μm, was assumed (see below).

Simulations indicated that the mean energy error between the energy profile at the screen and the initial one is always negligible (below 0.1 %). Figure 2 shows other important results. At 120 MeV, witness and driver can be distinguished

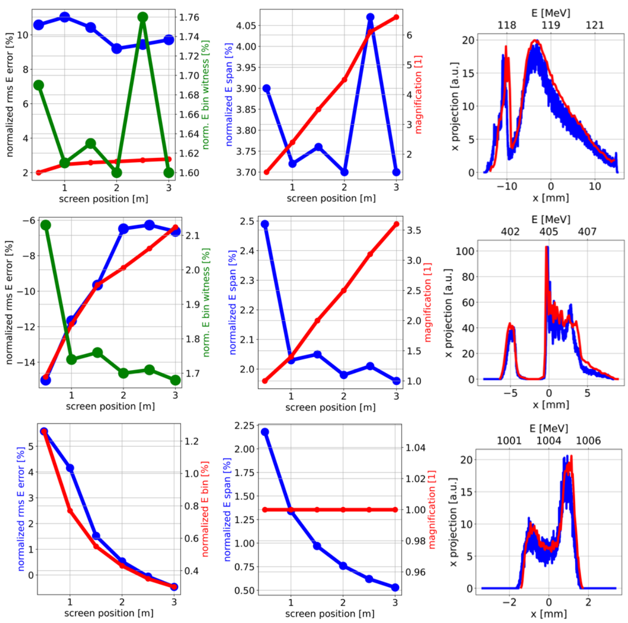

Figure 2: Simulation results for driver and witness at 120 MeV (top) and 400 MeV (middle), as well as for the witness at 1 GeV (bottom). Left: rms energy error versus the dipole-screen distance, for the witness (blue) and driver (red), normalized by the corresponding initial rms energy. The energy resolution normalized by the initial rms energy of the witness is in green. Middle: energy span (blue) normalized by the initial mean energy, and the required magnification (red). Right: FOV projection (blue) on the x axis, for the screen placed at 2 m. The energy axis is derived from the horizontal one. The initial energy profile is in red.

on the screens, respectively on the left and right. The screen at 2 m provides rms energy errors of 9 % (witness) and 3 % (driver), and energy resolutions of 1.6 % (witness) and 0.3 % (driver). The energy span is 4 %, and the magnification is 4.5 (30 mm of horizontal FOV). A lower dipole-screen distance would lower the required magnification, allowing the use of a smaller screen. If needed, it would also give more margin to increase the magnification by moving away the camera from the screen. At the same time, the energy resolution, span and rms error would not change significantly. Thus, lower distances are preferable, provided they are feasible in terms of mechanical constraints and emitted particle radiation.

At 400 MeV, witness and driver are separated on the screens (Fig. 2, middle right). Placing the screen at 2 m is a good choice, since the rms energy errors (6 % for witness, 9 % for driver), energy resolutions (1.7 % for witness, 0.5 % for driver) and magnitude (2.5) would be relatively low. The energy span would be 2 %, sufficient to deal with mean energy jitters estimated at 0.2 % [2]. The screen at 2 m would be a good solution also at 1 GeV, since the rms energy error and energy resolution would be below 1 %. However, a magnification of 1 would lead to an energy span of 0.8 % (Fig. 2, bottom middle), too small to contain the estimated mean energy jitter of 4 % at the exit of the plasma module [2]. With a magnification of 5.3, the energy span would increase to 4 %, but the energy bin size would grow to 2.4 %. The rms energy error would remain at 0.5 %.

DESIGN OF ENERGY MEASUREMENTS FOR SSRIP

The spectrometer of SSRIP (Fig. 3, top) is a sector dipole installed at the end of the beamline. To estimate the accuracy

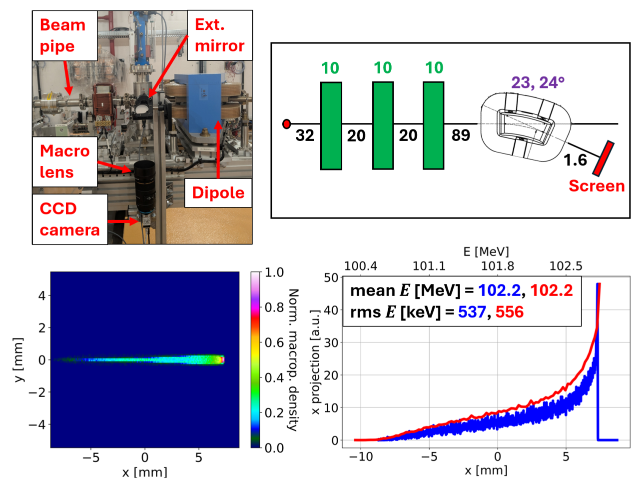

Figure 3: Top left: photo of the SSRIP spectrometer and of a diagnostics station used to measure the beam spot before the dipole. Top right: accelerator layout considered in simulation. The numbers indicate lengths in centimeters. The dipole arc length and bending angle are in purple, while the quadrupoles are in green. The red dot indicates where the simulation starts. Bottom left: screen FOV containing the beam spot. The magnification is 2.6. Bottom right: FOV projection (blue) on the x axis. The initial energy profile is in red. Mean and rms energies of the profiles are in the box.

and resolution of the energy measurements, simulations were performed with Elegant, starting at 11 m from the RF-gun cathode and ending at the screen 1.6 m far from the dipole exit. The initial bunch distribution was obtained from a separate simulation. The quadrupole strengths were found with MAD-X, aiming at minimizing β_x at the screen. The obtained strengths were within the limits set by the maximum quadrupole gradient. A camera sensor with 1920 × 1200 pixels, and pixel side of 3.45 μm, was assumed in simulation, since the installed camera has these features [11].

Figure 3 (bottom left) shows the FOV at the screen. The magnification of 2.6 provides an energy resolution of 0.2 %, with not more than 0.02 % of the macroparticles out of the

ISBN: 978-3-95450-262-2 ISSN: 2673-5350 doi: 10.18429/JACoW-IBIC2025-WEPCO05

FOV. The energy span is 2 %, while the mean and rms energy errors are respectively 0.01 % and 3 % (Fig. 3, bottom right). The macroparticle transverse displacements are always lower than half of the lattice aperture. All these results show that the spectrometer works as desired. Essentially the same outcomes were found turning off the quadrupoles, since the dipole weak focusing makes β_x already small at the screen.

CHARACTERIZATION OF THE CCD CAMERA-MACRO LENS SYSTEM

Measurements were performed to characterize the resolution and magnification of the optics system which will be used at SSRIP and EuPRAXIA@SPARC_LAB to acquire the beam spots. The system, made of a CCD camera [11] and a macro lens [12] (Fig. 4, left), was tested by using a resolution test target [13] back-lighted by an electroluminescent illuminator providing uniform light. The camera sensor has

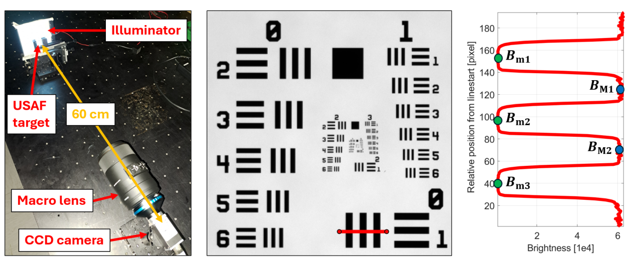

Figure 4: Left: measurements setup with a sensor-target distance of 60 cm. Middle: recorded USAF image. The red segment indicates where the pixel profiling is performed. Right: outcome of the pixel profiling. A 12-bit brightness value is associated to each pixel. The minimum and maximum brightness points are in green and blue, respectively.

1920 × 1200 pixels, with pixel side of R_0 = 3.45 µm. Different sensor-target distances were considered, from 50 cm to 130 cm. For each measurement, the exposure time was chosen to exploit the entire brightness range, without reaching saturation. The pylon Viewer software [14] was used to set the acquisition parameters and to save the images (Fig. 4, middle), which were then analyzed with Matlab [15] (Fig. 4, right). For each sensor-target distance, the resolution of the optics system was evaluated by pixel-profiling line-segment triplets of different target elements [13, 16, 17]. The thickness of a line segment corresponds to the resolution. For a given triplet, the Michelson Contrast [18] was computed for each of the four pairs of consecutive minima-maxima of the brightness curve (Fig. 4, right), and then an average was taken. The measurements also allowed to determine the magnification of the optics system, which depends on the sensor-target distance. The magnification was evaluated by dividing the known length of a segment by the product of R_0 and the number of pixels covered by the segment.

Figure 5 (left) shows the measured contrast as a function of the resolution. For a given contrast value, the resolution worsens with the sensor-target distance, and for a reference

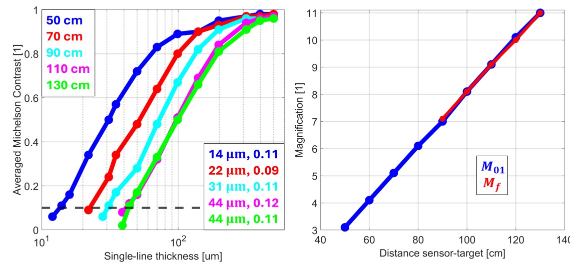

Figure 5: Left: measured contrast as a function of the target single-line thickness (resolution). Each color represents a different sensor-target distance (top-left box). The resolutions corresponding to a contrast of 0.1 (dashed line) are in the bottom-right box. Right: magnification as a function of the sensor-target distance. For each evaluation, the segment with known length is either a line segment belonging to the element 1 of group 0 (blue) or one side of the target (red).

contrast of 0.1 (as chosen in Refs. [16, 17]), the resolution is 14 µm at 50 cm. This resolution is 33 % larger than the expected one, i.e. the product of R_0 and the magnification of 3 at 50 cm (Fig. 5, right). The magnification increases linearly with the target-sensor distance, rising by one unit every 10 cm. Similar magnifications were found using either the longest line-segment of the target or one side of the target.

CONCLUSIONS

The design of the energy measurements to be performed at EuPRAXIA@SPARC_LAB revealed that the mean energy errors are negligible, while the rms energy errors can arrive up to 10 %. The most appropriate screen position was indicated for each spectrometer. At 120 MeV, the dipole-screen distance should be as low as possible, while at 400 MeV and 1 GeV placing the screen at 2 m provides a good solution. It was possible to measure driver and witness together on the screen, both at 120 MeV and 400 MeV. This will simplify significantly the setup of the energy measurements.

Simulations showed that the SSRIP spectrometer works as desired. With a magnification of 2.6 giving an energy span of 2 %, the mean energy error is negligible, and the rms error is just 3 %. Turning off the quadrupoles leads essentially to the same results, so quadrupoles could be kept off, which is a significant simplification of the measurements setup.

The optics measurements indicated that the resolution worsens for larger target-sensor distances. Setting a contrast of 0.1 as reference, the resolution at 50 cm is 14 µm, which is 33 % larger than the expected one. The magnification is 3 at 5 cm and increases by one unit every 10 cm of additional distance. Further studies are required to quantify the impact of the contrast values on the energy profiles at the screen.

ACKNOWLEDGMENTS

We thank A. Liedl for the information on the lattice apertures, and T. De Nardis, M. Galletti, G. Grilli, M. Marongiu, and D. Pellegrini for their help during the optics measurements.

ISBN: 978-3-95450-262-2 ISSN: 2673-5350 doi: 10.18429/JACoW-IBIC2025-WEPCO05

REFERENCES

[1] R. W. Assmann *et al.*, "EuPRAXIA Conceptual Design Report", *Eur. Phys. J. Spec. Top.*, vol. 229, no. 24, pp. 3675–4284, Dec. 2020. doi:10.1140/epjst/e2020-000127-8

[2] "EuPRAXIA@SPARC_LAB Technical Design Report", to be published.

[3] A. R. Rossi *et al.*, "Plasma Acceleration Experiment at SPARC_LAB with External Injection", in *Proc. IPAC'12*, New Orleans, LA, USA, May 2012, paper WEEPPB002, pp. 2169–2171. https://jacow.org/IPAC2012/papers/WEEPPB002.pdf

[4] F. Sannibale and M. Vescovi, "Linac to Accumulator Area Transfer Line (LAAT) & DAΦNE Linac Spectrometer DLS", DAΦNE Technical Note LC-3, Feb. 1992. https://www.lnf.infn.it/acceleratori/dafne/NOTEDAFNE/LC/LC-3.pdf

[5] K. Techakaew, K. Kongmali, and S. Rimjaem, "Electron Energy Spectrometer for MIR-THz FEL Light Source at Chiang Mai University", *Annu. Rev. Nucl. Part. Sci.*, vol. 6, no. 3, pp. 703–712, Jul. 2023. doi:10.3390/particles6030043

[6] S. Kasaei, Sh. Sanaye Hajari, M. Bahrami, and H. Shaker, "Spectrometer design for diagnostics in a wide range of energy at a linear accelerator", *J. Instrum.*, vol. 13, no. 06, pp. P06021–P06021, Jun. 2018. doi:10.1088/1748-0221/13/06/P06021

[7] J. O. Deasy, P. R. Almond, M. T. McEllistrem, and C. K. Ross, "A simple magnetic spectrometer for radiotherapy electron beams", *Biol. Med. Phys. Biomed. Eng.*, vol. 21, no. 11, pp. 1703–1714, Nov. 1994. doi:10.1118/1.597271

[8] F. Méot, *Understanding the Physics of Particle Accelerators*. Springer International Publishing, 2024. doi:10.1007/978-3-031-59979-8

[9] M. Borland, "elegant: A Flexible SDDS-Compliant Code for Accelerator Simulation", in *Proc ICAP'00*, Dramstadt, Germany, Sep. 2000. doi:10.2172/761286

[10] MAD-X code, https://madx.web.cern.ch/

[11] CCD camera Basler ace 2 a2A1920-51gmBAS, https://www.baslerweb.com/it-it/shop/a2a1920-51gmbas/

[12] SIGMA MACRO 105mm F2.8 EX DG OS HSM, https://www.sigma-global.com/en/lenses/105_28_os

[13] THORLABS 1951 USAF Resolution Test Target (1" × 1"), https://www.thorlabs.com/newgrouppage9.cfm?objectgroup_id=4338

[14] Basler Pylon Viewer software, https://www.baslerweb.com/it-it/software/pylon/pylon-viewer

[15] MATLAB programming language, https://it.mathworks.com/products/matlab.html

[16] F. Cioeta *et al.*, "Spot Size Measurements in the ELI-NP Compton Gamma Source", in *Proc. IBIC'16*, Barcelona, Spain, Sep. 2016, pp. 532–535. doi:10.18429/JACoW-IBIC2016-TUPG74

[17] M. Marongiu *et al.*, "Optical Issues for the Diagnostic Stations for the ELI-NP Compton Gamma Source", in *Proc. IPAC'17*, Copenhagen, Denmark, May 2017, pp. 238–241. doi:10.18429/JACoW-IPAC2017-MOPAB058

[18] A.A. Michelson, *Studies in Optics*. Chicago, IL, USA: University of Chicago Press, 1927. https://books.google.it/books?id=FXFTnQEACAAJ